



ARL-TR-7663 • MAY 2016



Pyroelectric Energy Harvesting: Model and Experiments

by Felisa Sze and Brendan Hanrahan

NOTICES

Disclaimers

The findings in this report are not to be construed as an official Department of the Army position unless so designated by other authorized documents.

Citation of manufacturer's or trade names does not constitute an official endorsement or approval of the use thereof.

Destroy this report when it is no longer needed. Do not return it to the originator.

ARL-TR-7663 • MAY 2016



Pyroelectric Energy Harvesting: Model and Experiments

by Felisa Sze and Brendan Hanrahan
Sensors and Electron Devices Directorate, ARL

REPORT DOCUMENTATION PAGE				Form Approved OMB No. 0704-0188	
<p>Public reporting burden for this collection of information is estimated to average 1 hour per response, including the time for reviewing instructions, searching existing data sources, gathering and maintaining the data needed, and completing and reviewing the collection information. Send comments regarding this burden estimate or any other aspect of this collection of information, including suggestions for reducing the burden, to Department of Defense, Washington Headquarters Services, Directorate for Information Operations and Reports (0704-0188), 1215 Jefferson Davis Highway, Suite 1204, Arlington, VA 22202-4302. Respondents should be aware that notwithstanding any other provision of law, no person shall be subject to any penalty for failing to comply with a collection of information if it does not display a currently valid OMB control number.</p> <p>PLEASE DO NOT RETURN YOUR FORM TO THE ABOVE ADDRESS.</p>					
1. REPORT DATE (DD-MM-YYYY) May 2016	2. REPORT TYPE Final	3. DATES COVERED (From - To) 07/2015–02/2016			
4. TITLE AND SUBTITLE Pyroelectric Energy Harvesting: Model and Experiments			5a. CONTRACT NUMBER		
			5b. GRANT NUMBER		
			5c. PROGRAM ELEMENT NUMBER		
6. AUTHOR(S) Felisa Sze and Brendan Hanrahan			5d. PROJECT NUMBER		
			5e. TASK NUMBER		
			5f. WORK UNIT NUMBER		
7. PERFORMING ORGANIZATION NAME(S) AND ADDRESS(ES) US Army Research Laboratory ATTN: RDRL-SED-E 2800 Powder Mill Road Adelphi, MD 20783-1138			8. PERFORMING ORGANIZATION REPORT NUMBER ARL-TR-7663		
9. SPONSORING/MONITORING AGENCY NAME(S) AND ADDRESS(ES)			10. SPONSOR/MONITOR'S ACRONYM(S)		
			11. SPONSOR/MONITOR'S REPORT NUMBER(S)		
12. DISTRIBUTION/AVAILABILITY STATEMENT Approved for public release; distribution unlimited.					
13. SUPPLEMENTARY NOTES					
14. ABSTRACT Efficient pyroelectric energy conversion would enable portable, wireless power generation capabilities for the Army. This technology relies on the pyroelectric effect in ceramic materials, where the dielectric polarization has a strong temperature dependence. In order to evaluate pyroelectric systems, one must precisely measure and control electric field and temperature while evaluating alternating pyroelectric currents. This technical report describes the modeling, assembly, and performance of a custom pyroelectric energy conversion testing system. This system is used to evaluate a lead zirconate titanate thin film pyroelectric capacitor as an energy conversion system. The conversion cycle and future outlook are presented.					
15. SUBJECT TERMS pyroelectric, energy harvesting					
16. SECURITY CLASSIFICATION OF: Unclassified		17. LIMITATION OF ABSTRACT UU	18. NUMBER OF PAGES 44	19a. NAME OF RESPONSIBLE PERSON Brendan Hanrahan	
a. REPORT Unclassified	b. ABSTRACT Unclassified	c. THIS PAGE Unclassified	19b. TELEPHONE NUMBER (Include area code) 301-394-1960		

Contents

List of Figures	iv
Acknowledgments	vi
Summary	vii
1. Introduction	1
2. Modeling	4
3. Hardware	11
3.1 Temperature Actuation and Measurement	11
3.2 Instruments	13
4. Software	13
4.1 Heater Control	13
4.2 Electric Field Control	16
4.3 Data Acquisition	16
4.4 Synchronization	18
4.5 Saving Data	20
5. Results	20
5.1 Static Testing	20
5.2 Temperature Characterization	23
5.3 Pyroelectric Current	25
5.4 Pyroelectric Energy Conversion Cycle Testing	27
6. Conclusion and Future Outlook	30
7. References	32
Distribution List	39

List of Figures

Fig. 1	Schematic of a pyroelectric conversion cycle with a description of each of the processes.....	1
Fig. 2	Polarization hysteresis loops for 30:70 composition PZT thin films taken over the range of 26–166 °C	2
Fig. 3	Remnant polarization vs. temperature over the tested range	3
Fig. 4	Pyroelectric element model consisting of a current source for the pyroelectric current, a dielectric capacitor for the adiabatic charging and discharging, and optionally a resistor to include leakage current ..	4
Fig. 5	Hysteresis loops at different temperatures. Red is a hot temperature, blue is a cold temperature. The Brayton cycle can be estimated from these static measurements.....	5
Fig. 6	Schematic of current amplifier with a pyroelectric element model	6
Fig. 7	A comparison of actual pyroelectric data measured taken from (Bhatia, Damodaran et al. 2014) (right) with a current amplifier and the simulation with the same parameters (left).....	8
Fig. 8	The simulation model with a subcircuit that is the equivalent to a time-variable resistor, as the value of resistance is dependent on the voltage source which itself is time varying	10
Fig. 9	Simulation results from the model in Fig. 8. The resistance and the capacitance changed gradually with the temperature change, but with the electric field, the resistance changed suddenly. The pyroelectric current is included as well but is too low to be visible with leakage current present.....	10
Fig. 10	Schematic of the testing setup. The probe station contains the heater, sample, and RTD chip, and connections to those components are done through probes. The types of connections between components are included.....	12
Fig. 11	Heater control subprocess. The beginning is the initialization process, and the colored boxes highlight the 3 different modes.....	15
Fig. 12	The data acquisition subprocess. There is initialization in the beginning before the DAQ continuously takes readings that are then processed during the run and saved in the end.	17
Fig. 13	Electric field subVI timing. The orange boxes are actual subVIs, while black boxes represent how long they take to occur.	19

Fig. 14	Two hysteresis loops at a cold temperature and a hot temperature. The upper curves of the loops between points 1 and 2, and 3 and 4 represent the adiabatic charging and discharging of the Brayton cycle, while the differences in the loops at a constant voltage between points 2 and 3, and 4 and 1 represent the isolectric heating and cooling.....	21
Fig. 15	Capacitance versus voltage for the pyroelectric sample at the cold temperature	22
Fig. 16	The leakage current of the pyroelectric sample at the cold temperature. The heating rate has to be fast enough to have the pyroelectric current be visible past the leakage current.	23
Fig. 17	Resistance and temperature over time. The humps highlighted in the beginning of the resistance plot is caused by poor contact between the probes and the RTD chip.	24
Fig. 18	Pyroelectric current with triangle temperature waveform. It is clear that it is pyroelectric because it is consistently the expected shape, it is about 90° out of phase with the temperature, and it is on the order of magnitude expected.	26
Fig. 19	A graph of the Brayton cycle. The Brayton cycle output is the voltage output of the current amplifier, so it shows the shape of the output current but not the exact value. The applied voltage is for the electric field.	27
Fig. 20	Brayton cycle current, specifically the pyroelectric current. The spikes from the adiabatic charge and discharge are not shown in full. The temperature curve is shown as well. Some data were discarded due to voltage spikes occurring when the current amplifier changes gain.	28
Fig. 21	Brayton cycle current, specifically the dielectric charge and discharge events. The currents at those points are incorrect, as the voltage output was clipped there. Some data were discarded due to voltage spikes occurring when the current amplifier changes gain.	29
Fig. 22	Pyroelectric energy conversion loop calculated from current measurements.....	30

Acknowledgments

We would like to thank Mr Nick Jankowski and Dr Andrew Smith for their advice regarding the thermal design of the test setup. We would also like to thank Dr Sarah Bedair and Dr Nathan Lazarus for their helpful discussions regarding the circuit modeling and electrical subsystem.

Summary

This report describes the modeling, assembly, and initial testing results of a custom experimental setup dedicated to evaluating pyroelectric energy conversion (PEC). The pyroelectric property provides an energy transduction mechanism between thermal and electrical domains in materials with a temperature-dependent polarization. Pyroelectricity could, therefore, be used in power generation, wireless power, and Army cooling applications. To date, there have been very few examples of measured energy conversion in pyroelectric materials, yet thermodynamic modeling of these systems suggests that there could be high efficiencies, particularly around material phase transitions. In order to evaluate these models and the future application potential of this technology, PEC needs to be evaluated in operando. A test bed that can precisely apply synchronous electric field and temperature waveforms while measuring pyroelectric current has been created. Energy conversion was performed on a lead zirconate titanate thin film material, which is a leading candidate for future PEC application. The results suggest some disagreement between modeled and measured pyroelectric coefficients, but point toward system improvements to improving the measurement accuracy and power output of future PEC applications.

INTENTIONALLY LEFT BLANK.

1. Introduction

Efficient, compact thermal-to-electric energy conversion schemes could be used for portable or wireless power generation, as well as solid state cooling. Among potential technologies, such as thermoelectrics or thermionics, pyroelectric energy conversion remains the least understood but has significant potential. One of the crucial missing pieces toward realizing a pyroelectric energy converter (PEC) is in evaluating pyroelectric materials in operando, rather than calculating energy conversion metrics from static materials properties. This report describes the modeling, assembly, and execution of a pyroelectric energy conversion testing setup.

The PEC mechanism relies on the temperature dependence of the dielectric displacement (polarization) in a piezoelectric material. To extract work from the pyroelectric effect, the material acts as the dielectric in a capacitor that is charged by an external electric field. Then the charged capacitor is heated and the pyroelectric evolution of charge pushes current through the circuit, proportional to the heating rate and pyroelectric constant. The hot pyroelectric material is discharged electrically then cooled, resulting in current flow in the opposite direction, returning to its original state. This thermodynamic process is described schematically in Fig. 1.

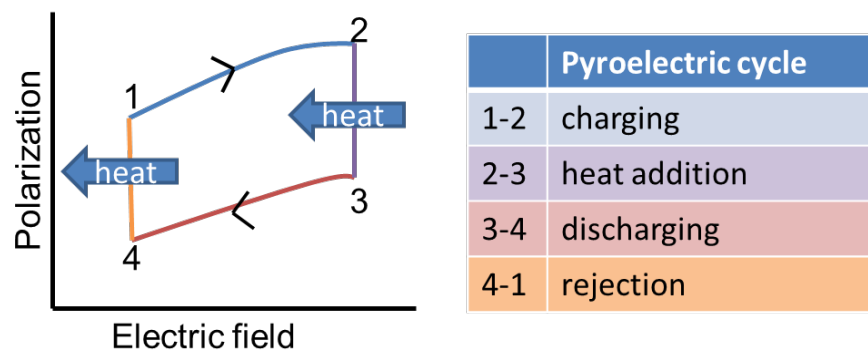


Fig. 1 Schematic of a pyroelectric conversion cycle with a description of each of the processes

The area encompassed by the cycle shown in Fig. 1 is equivalent to the energy density of the process. The change in polarization with temperature (pyroelectric effect) and the electric field should be maximized to maximize work. This cycle, among others, was first described by Olsen et al. (1985), who determined an Ericsson-equivalent pyroelectric cycle was the best balance between work output and feasibility. An in-depth thermodynamic analysis of the Olsen cycle was performed by Sebald and colleagues in 2009, establishing the heat, entropy, and

work relationships for each of the pyroelectric processes (Sebald G, Pruvost S, Guyomar, D 2008, Sebald G, Guyomar D, Agbossou A 2009). Recently, Jankowski proposed using a Brayton cycle for energy conversion, which uses adiabatic instead of isothermal charging and discharging, as the Olsen does. We showed that this cycle was more efficient than the Olsen cycle at the expense of work, but the cycle was able to be run at higher frequencies, which ultimately results in high power densities (Jankowski N, Smith A, Hanrahan B 2016).

The measurement of pyroelectric properties can be performed by direct or indirect methods. Commonly, polarization hysteresis loops are taken at different temperature baselines, and then the relationship between polarization and temperature can be interpolated. This type of measurement is shown in Fig. 2.

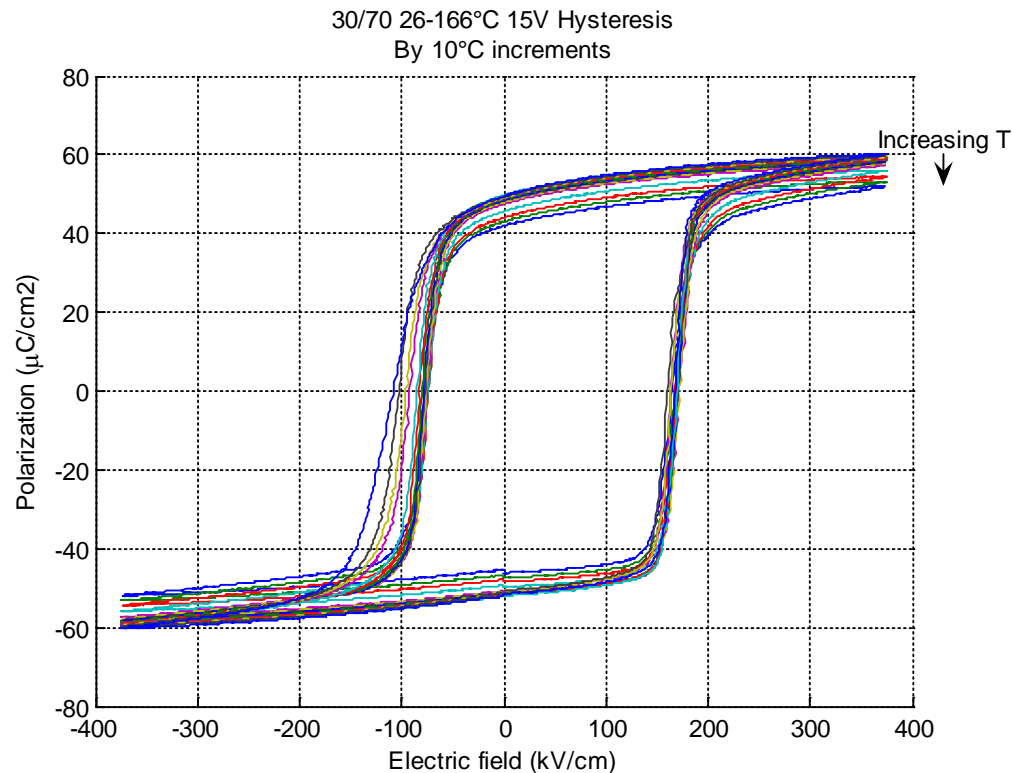


Fig. 2 Polarization hysteresis loops for 30:70 composition PZT thin films taken over the range of 26–166 °C

From these measurements, the polarization vs. temperature relationship can be graphed as shown in Fig. 3.

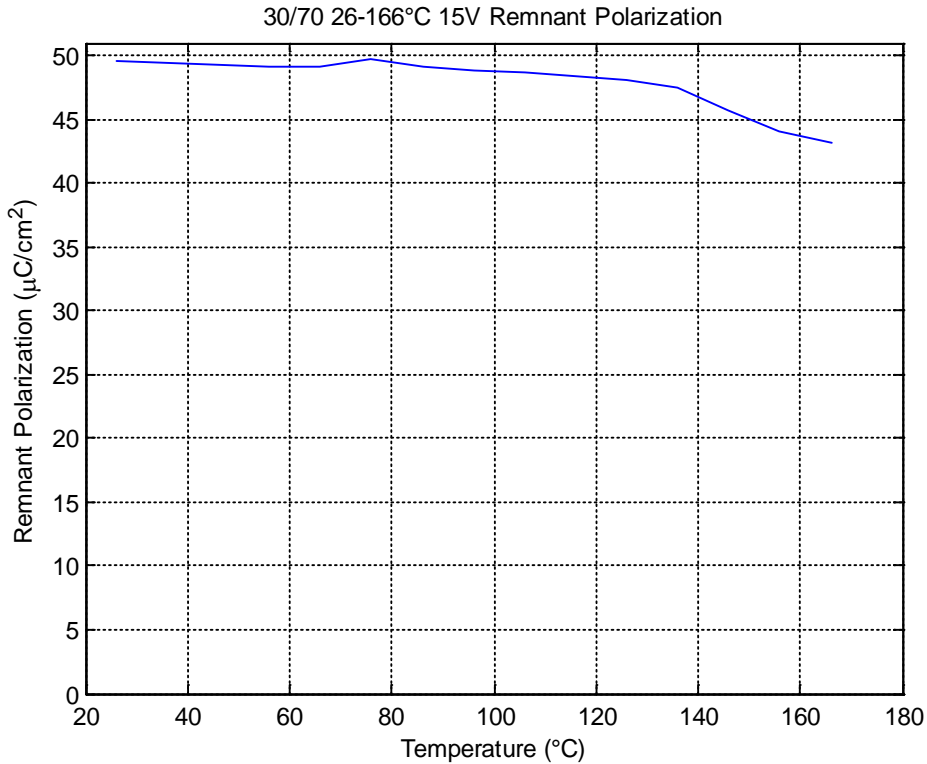


Fig. 3 Remnant polarization vs. temperature over the tested range

The temperature-polarization value at various applied fields can be interpolated from the hysteresis data. The benefit of this approach is that the system temperature can be well established.

The direct measurement of pyroelectric current is a closer analog to the operation of a PEC system, so the values gained from this measurement will have more relevance for this application. Generally, any current measurement of a pyroelectric capacitor under dynamic temperatures is a direct measurement. The difference among techniques depends on heating frequency. Bhatia et al. (2014) explored a range of frequencies measurements from 0.2 Hz to 1.3 MHz and found higher fidelity in the faster measurements because of the reduced influence of leakage current.

There have only been a handful of attempts at making a real generator (Navid A, Vanderpool D, Bah A, Pilon L 2010, Lee FY, Jo HR, Lynch CS, Pilon L 2013). It is not well understood how well the simulated conversion cycles correlate with directly measured cycles in thin films. This issue has been explored in the similar field of electrocalorics, but there is disagreement between those who think it does closely correlate.

2. Modeling

The pyroelectric energy cycle was modeled using OrCAD PSpice software to design the system and predict the energy conversion results. The performance of the model was compared to data taken from (Bhatia, Damadoran Cho, Martin, King 2014) about pyroelectric energy conversion measured with a current amplifier to judge the model's accuracy.

Two methods of measuring pyroelectric behavior are with the Sawyer-Tower circuit and with a current amplifier; both methods were initially modeled before the current amplifier was chosen for the setup.

The pyroelectric element is commonly modeled as a dielectric capacitor and a current source in parallel, as seen in Fig. 4 (Batra AK, Bandyopadhyay A, Chilvery AK, Thomas M 2013, Xie J. et. al. 2010). The dielectric capacitor represents the behavior seen during charging and discharging, and the current source represents the pyroelectric current from the heating and cooling. A resistor can also be added in parallel to represent leakage current present in the capacitor.

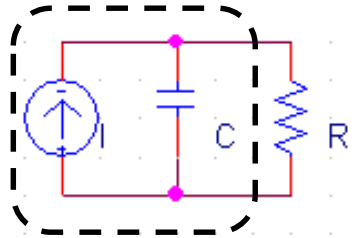


Fig. 4 Pyroelectric element model consisting of a current source for the pyroelectric current, a dielectric capacitor for the adiabatic charging and discharging, and optionally a resistor to include leakage current

In general, the dielectric capacitor would be seen in effect only when the electric field changes, and the current source seen only during the temperature change. However, the capacitance of the pyroelectric element is affected by the change in temperature, and the leakage current is affected by changes in both the electric field and temperature.

To model a specific pyroelectric element's performance through the Brayton cycle, one must understand the temperature- and electric field-dependent properties. To obtain this information, the capacitance is measured for the dielectric capacitor part of the model, and hysteresis loops at 2 different temperatures are needed to determine the total output currents of the Brayton cycle and the pyroelectric currents. The heating rate of the system is needed for the timing of the cycle, as well as the expected pyroelectric current. The relationship between the hysteresis loops and temperature is shown in Fig. 5.

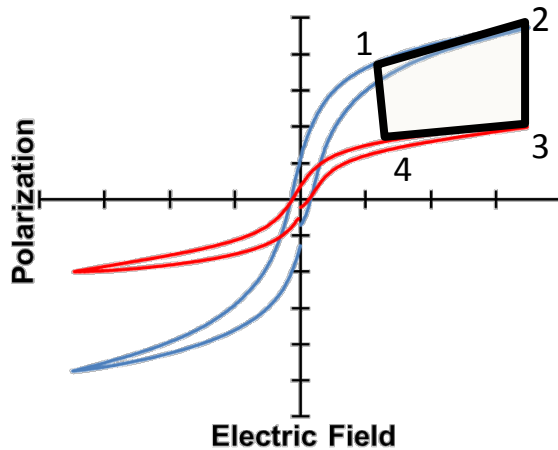


Fig. 5 Hysteresis loops at different temperatures. Red is a hot temperature, blue is a cold temperature. The Brayton cycle can be estimated from these static measurements.

The top legs of the hysteresis loops in the first quadrant of Fig. 5 represent the adiabatic charging and discharging legs of the Brayton cycle, while the difference in displacements at the same electric field at different temperatures gives an estimation of the change in charge during an isoelectric heat addition/rejection leg. Multiplying the difference in displacements by the area of the pyroelectric element gives the total charge change, and dividing the change in charge by the time it would take the heating element to go from one temperature to the other gives the total output current expected during that isoelectric step.

These output currents do not consist only of pyroelectric currents. The change in capacitance due to the change in temperature has to be taken into account as well. That resulting current can be estimated as

$$i_c(\theta) = \frac{\Delta C}{\Delta t} V, \quad (1)$$

where ΔC is the change in capacitance, Δt is the amount of time needed to change temperatures, and V is the voltage on the pyroelectric element that causes the constant electric field during either steps 2 to 3 or steps 4 to 1, as determined by the thickness of the pyroelectric capacitor.

The pyroelectric current represented by the current source can then be determined as follows:

$$\frac{A \Delta D(\theta)}{\Delta t} - \frac{\Delta C}{\Delta t} V = \frac{A \Delta P_r(\theta)}{\Delta t} = i_p(\theta), \quad (2)$$

where $\Delta D(\Theta)$ is the total change in displacement due to temperature, and $\Delta P_r(\Theta)$ is the change in remnant polarization due to temperature.

An alternative to using 2 hysteresis loops to determine the total displacement and current during the heating and cooling of the cycle is to estimate the pyroelectric currents as follows:

$$i_p(\theta) = pA \frac{dT}{dt}, \quad (3)$$

where p is the pyroelectric coefficient of the pyroelectric element, A is the area, and dT/dt is the rate of change of the temperature during the cycle. The pyroelectric coefficient can be obtained from the slope of the remnant polarization versus temperature data through the temperature range used. The estimation of the current from the capacitor during the isoelectric steps would remain the same, so the total current would be the pyroelectric current plus the dielectric current.

The pyroelectric element's performance through the Brayton cycle can be estimated by combining the dielectric capacitor, current source, and resistor into the current amplifier, changing the voltage source to represent changing electric field, and changing the capacitance and turning on the current source to represent changing temperature, with the current source having the appropriate values and timing to model the pyroelectric current, shown schematically in Fig. 6.

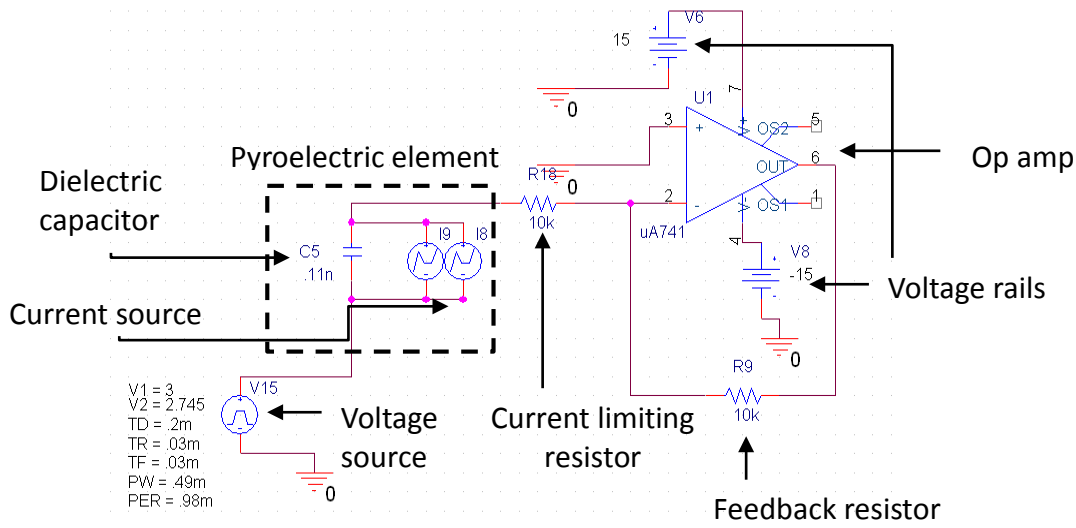


Fig. 6 Schematic of current amplifier with a pyroelectric element model

Current amplifiers are one way to measure current. They use an op-amp to establish a virtual ground at one input, such that a current sinking in that input is then sourced in a feedback circuit into the output of the op-amp. Putting a resistor in the feedback circuit allows the current to be converted into a voltage at the output of the op-amp, which can be used to determine the current value, as the resistor value will be a

gain. The current-limiting resistor present in the schematic is not needed normally but is used to make simulation possible.

Pyroelectrics are characterized by how the charge on their surface moves. As temperature changes, current amplifiers can be used to measure the pyroelectrics' performance by measuring the current that is produced as the pyroelectric goes through an energy harvesting cycle, such as the Olsen cycle.

The alternative to the current amplifier, the Sawyer-Tower circuit, consists of a large dielectric capacitor in parallel with the pyroelectric capacitor that integrates the current from the pyroelectric element. The voltage of the dielectric capacitor will then be in proportion to the charge on the pyroelectric capacitor. However, there exists the possibility of back voltage and parasitic capacitance skewing results, so the current amplifier is used instead.

To test the accuracy of the current amplifier and pyroelectric model, the model was simulated using characteristics and parameters matching that of actual experimental data. The results are shown in Fig. 7.

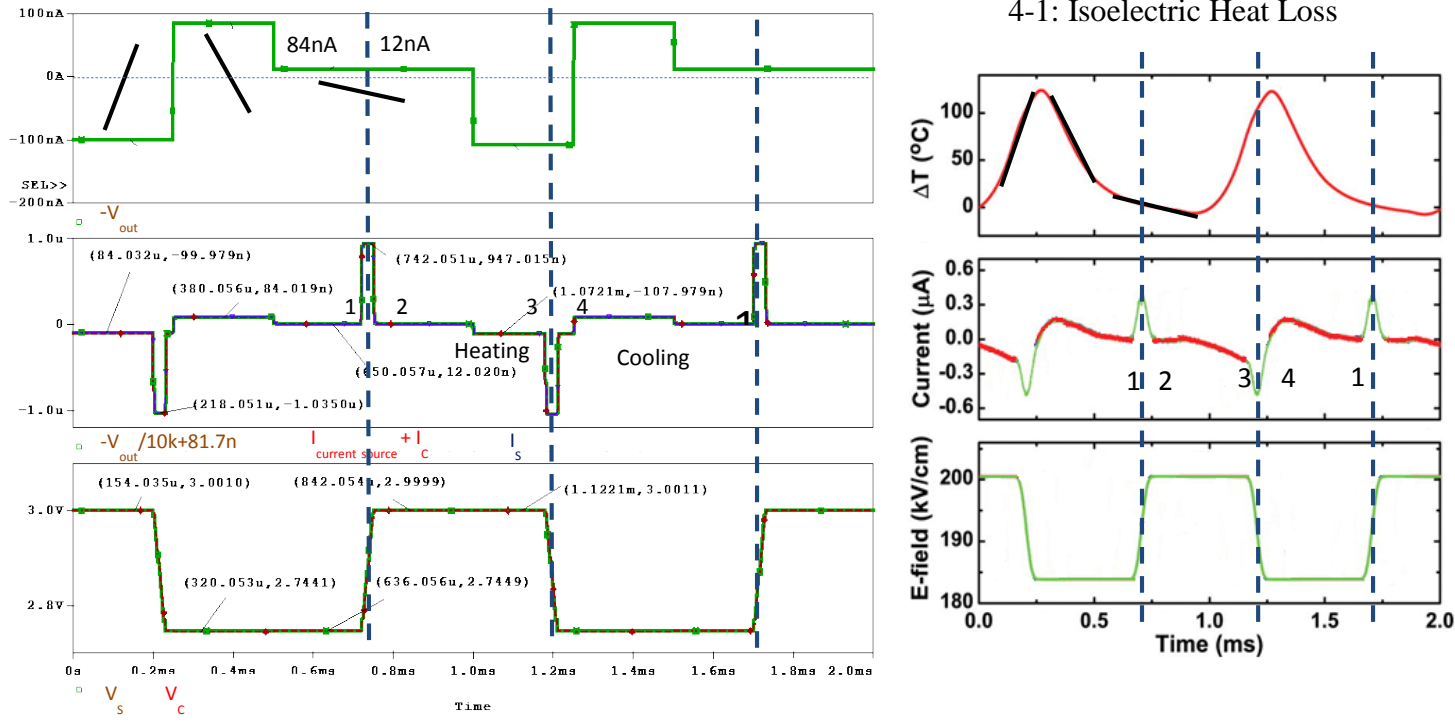


Fig. 7 A comparison of actual pyroelectric data measured taken from (Bhatia B, Damodaran AR., Cho H, Martin LW, King WP 2014) (right) with a current amplifier and the simulation with the same parameters (left)

NOTE: (Source: Bhatia, B. et. al. High-frequency thermal-electrical cycles for pyroelectric energy conversion. *J. Appl. Phys.* 2014;116:194509)

In Fig. 7, the rate of change for temperature in the data was simplified to linear segments to make modeling the pyroelectric current source more straightforward. The area, pyroelectric coefficient, and other characteristics of the pyroelectric capacitor were given within the data and were used to complete the model, as seen in Fig. 6.

There is good agreement between the simulated and published conversion cycles. Between points 1 and 2, isothermal charging, there is a positive spike in current from the capacitor charging due to the change in electric field. There is then heating between points 2 and 3, adiabatic heat addition, that causes a negative current, which leads into a more negative current spike caused by the isothermal discharging between points 3 and 4. Cooling then causes a positive current between points 4 and 1.

The magnitudes of the currents differ between the simulation and the data. The pyroelectric current in the simulation is less than in the data, and the dielectric current is greater in the simulation. A number of factors could have caused this, including not taking the change in capacitance and pyroelectric coefficient with temperature into account, and not including leakage current in the model.

Leakage current is caused by the pyroelectric capacitor having a finite resistance and current passing through due to Ohm's law. The resistance is dependent on the electric field and the temperature, and will decrease as either factor increases, meaning the leakage current increases with the electric field and temperature. The leakage current will then vary during the Brayton cycle and be greatest at point 3, where electric field and temperature are both high. Leakage current can be added to the pyroelectric model by adding a resistor in parallel.

OrCAD PSpice does not have a time variable resistor component available, so the Analog Behavioral Library can be used to create an equivalent component. It samples the current through its terminals and converts it to a voltage with galvanic insulation that follows Ohm's law, with the resistance value dependent on the voltage source. Figure 8 shows the component added to the pyroelectric element. When a resistor is added in parallel to the dielectric element, the theoretical leakage current is large enough to hide the pyroelectric effect if the rate of change of temperature is too slow. During isothermal charge and discharge, the leakage current increases and decreases linearly, respectively. During isoelectric heat addition and loss, the leakage current changes following the relation $1/x$, since by Ohm's law, the resistance is changing while the voltage is constant. Figure 9 shows this relationship.

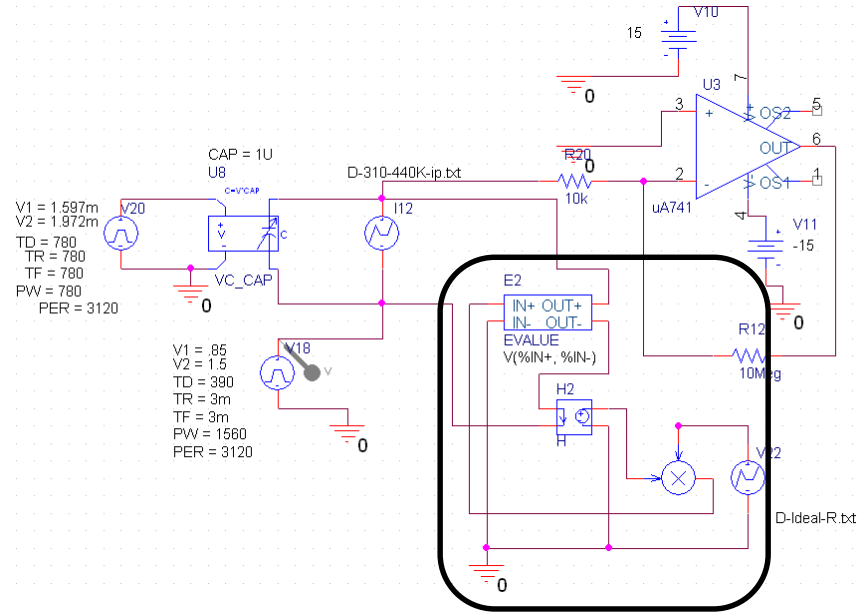


Fig. 8 The simulation model with a subcircuit that is the equivalent to a time-variable resistor, as the value of resistance is dependent on the voltage source which itself is time varying

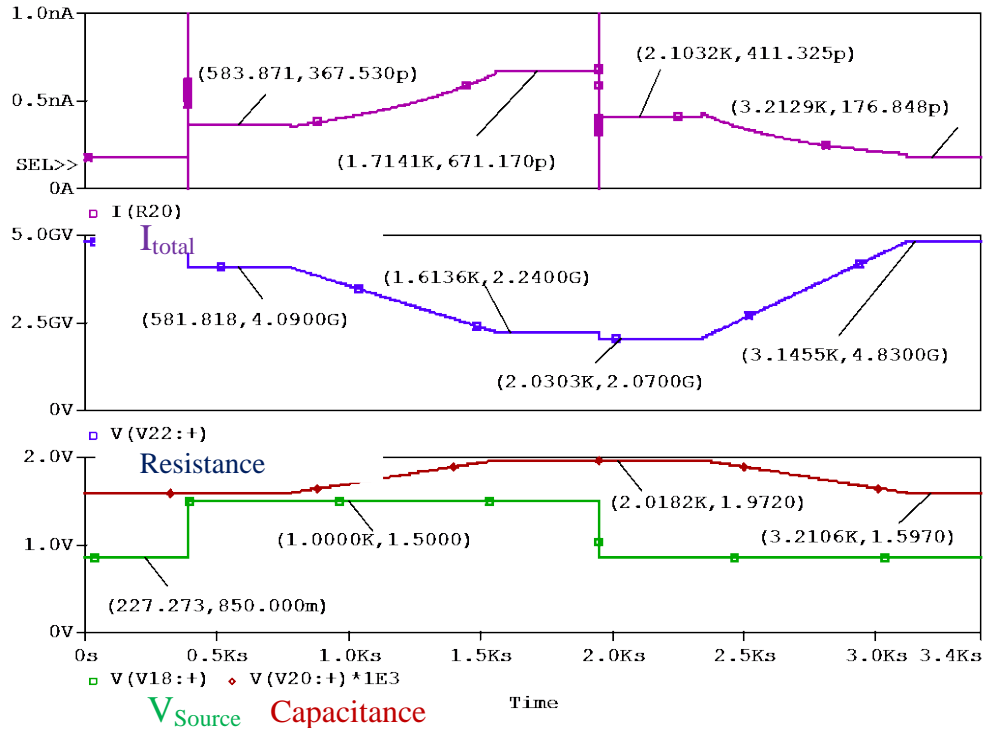


Fig. 9 Simulation results from the model in Fig. 8. The resistance and the capacitance changed gradually with the temperature change, but with the electric field, the resistance changed suddenly. The pyroelectric current is included as well but is too low to be visible with leakage current present.

In the future, the current could be integrated to obtain charge, then divided by the pyroelectric element's area to get displacement, and the displacement-electric field plot could be back-calculated. This could then be compared to the isothermal hysteresis loops of the actual sample.

3. Hardware

The pyroelectric testing setup consists of multiple capabilities to control and monitor temperature, electric field, and current. A computer is used to communicate and control the instruments. A Lakeshore Model TTPX Probe Station is used to house the pyroelectric sample and to set the baseline temperature, which is controlled by a Lakeshore Model 336 Temperature Controller. A 2 cm^2 secondary ceramic heater chip is used in series with the probe station to increase the dT/dt capabilities of the setup. To collect measurements and control the electric field on the sample, the Personal DAQ/3001, a data acquisition device, is used. A SR570 Current Amplifier is used to read the current output from the sample. Connections between the hardware are as seen in Fig. 10.

3.1 Temperature Actuation and Measurement

The pyroelectric sample is set on top of a ceramic resistive heater with a fast heating rate ($>1^\circ/\text{s}$), which, itself, is placed on top of the probe station sample stage. The stage then acts as thermal ground for the ceramic heater. A thin film metal trace on a silicon chip is used as a resistance temperature detector (RTD) and placed adjacent to the pyroelectric device on top of the ceramic heater element. It is assumed to be at the same temperature of the sample and its resistance is used to determine the sample temperature. A voltage divider circuit was used to read the resistance, and the voltages are read by the DAQ. An Agilent DC power supply powers the ceramic heater element up to 40 W.

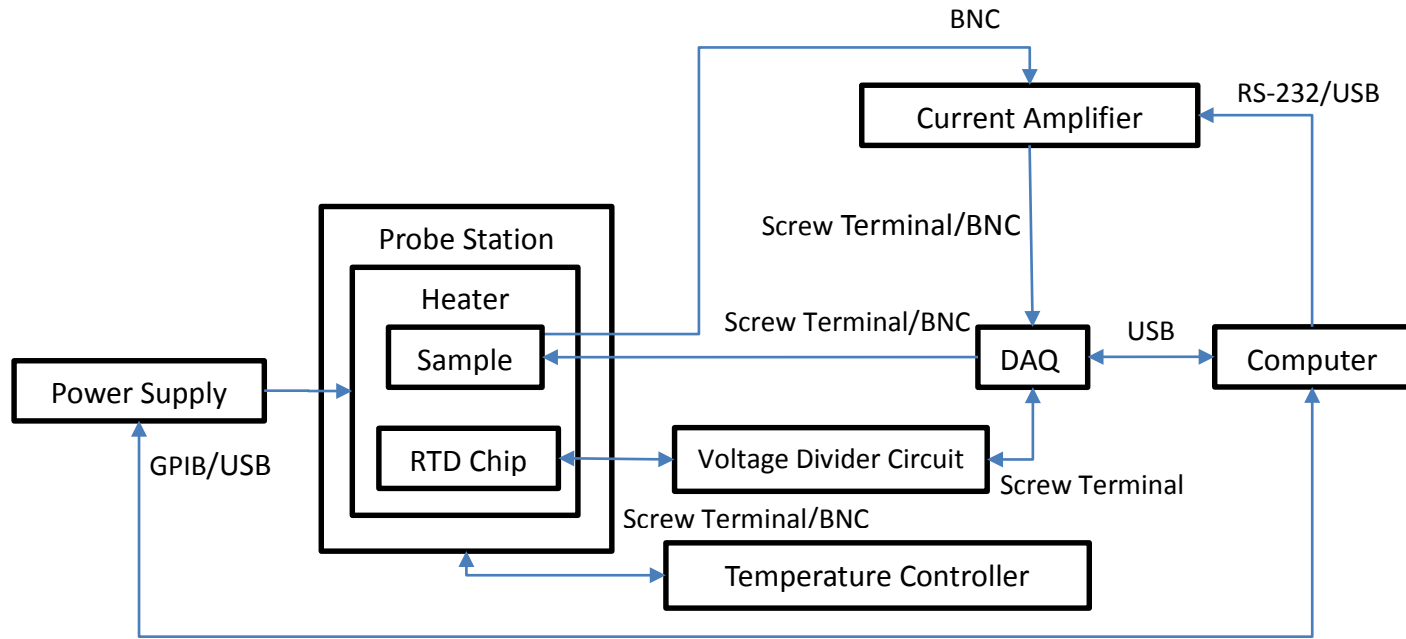


Fig. 10 Schematic of the testing setup. The probe station contains the heater, sample, and RTD chip, and connections to those components are done through probes. The types of connections between components are included.

3.2 Instruments

The Lakeshore Model TTPX Probe Station is used to control the environment of the energy conversion experiments. It is used in conjunction with the Lakeshore Model 336 Temperature Controller, which both measures and controls the temperature of multiple locations, including the sample stage, which, in this case, is the high-temperature sample stage. Model ZN50R-CVT temperature-variable probes are used to accommodate for sample thermal expansion without damaging the sample surface. The temperature controller is used to set a baseline temperature for the ceramic heater by providing heating against liquid nitrogen cooling.

Static characterization of the pyroelectric sample was performed with a Radian Precision Premier II Ferroelectric Tester. The Radian Vision software enables many electrical measurements including ferroelectric hysteresis loops, leakage, and capacitance tests. The Radian system uses a current amplifier to take measurements. It also communicates with the Lakeshore Model 336 temperature controller to enable automated isothermal ferroelectric materials characterization.

The pyroelectric conversion cycle instruments are controlled by the computer through custom LabVIEW software described in the following section. The DAQ is a USB module, while the current amplifier and the power supply uses RS-232 and general purpose interface bus for communication, respectively. All 3 have LabVIEW drivers available.

The equipment had a number of specific input and output requirements. The DAQ needed low noise inputs and high enough bandwidth for fast conversion cycles. It also needed analog outputs to cut down the number of individual voltage sources. The current amplifier needed low noise for low current measurements and changeable gain, since the expected currents vary by orders of magnitudes. The power supply needed high enough voltage for fast heating cycles.

4. Software

The software that controls the pyroelectric testing setup consists of a LabVIEW program split into multiple parallel processes. These include the control of the heater and the electric field, the acquisition by the DAQ, and the current amplifier.

4.1 Heater Control

A ceramic heater element, powered by a DC power supply, is used to modulate the temperature in the pyroelectric experiments. The heater is controlled in LabVIEW through the use of subprogram virtual instruments (VIs) specific to the DC power

supply. Communication is first established between the computer and the power supply, then the initial settings are exchanged, which include the initial voltage for the heater and current limits. The output is initially disabled so the resistive heater does not automatically start heating with the program start. The ‘Start Heat’ button enables the initial output. The heater control process is outlined in Fig. 11.

There are 3 modes for controlling the heater: Manual, Temp, and Timed. Manual mode lets the user control the heater by pressing the ‘Heat Off’ button repeatedly to disable and enable the voltage to the heater. Temp mode actively controls heater power to cycle between user-defined high and low temperatures. The power supply will remain on until the high temperature threshold is crossed, then it will turn off and the system will cool toward the low temperature set-point. Once the low temperature threshold is crossed, the power supply will be turned on to continue the cycle. Timed mode first lets the temperature reach one of the thresholds. After a threshold is reached, the program then goes into periodic heating cycles determined by the user inputs ‘Period’ and ‘Duty,’ which determine the cycle time and duty cycle, respectively. Pressing the ‘Heat Off’ button during the first step will also begin periodic cycling. There is a user input labeled ‘Heater Ctrl’ to change between modes. Power to the heating element is determined by the voltage setting. To update the voltage for the heater, there are inputs available, and a ‘Change Voltage’ button.

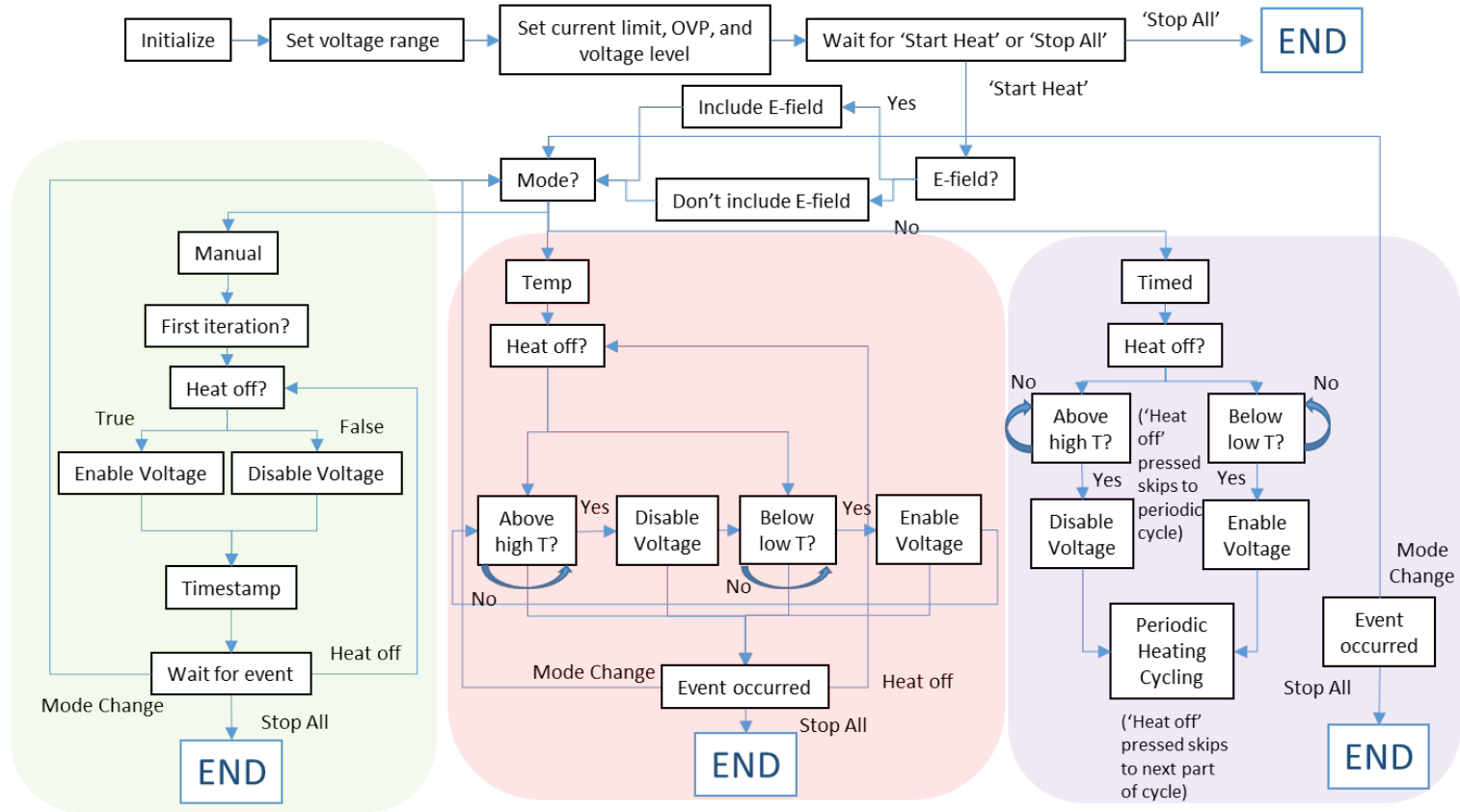


Fig. 11 Heater control subprocess. The beginning is the initialization process, and the colored boxes highlight the 3 different modes.

4.2 Electric Field Control

An electric field is applied to the sample for the energy conversion process. The field is applied by the DAQ card and controlled in the LabVIEW software. The timing of the electric field is automatically linked to the heater power state, regardless of heating mode. The ‘E-field?’ button toggles the application of the electric field during the heating cycles. The magnitude of the electric field is user defined in the “Voltage output” tab on front panel. The system is currently limited by the DAQ to 10 V max.

The pyroelectric conversion cycle generally includes synchronous charging-discharging and heating-cooling cycles. The expected current levels for different processes can vary by many orders-of-magnitude, depending on the size of the capacitor, heating rates, etc., so the current measurement needs to accommodate a wide range of magnitudes. To accomplish this, mid-process amplification changes of the current measurement are synchronized with the heating cycle. The goal is to minimize the amount of dead time caused by gain changes. The delay times can be manipulated from the front panel for debugging purposes, and the results can be observed in real-time.

4.3 Data Acquisition

Multiple data streams are needed to understand the performance of the pyroelectric conversion for a given set of conditions. These include current, resistance (for temperature), and electric field. Figure 12 illustrates the process of acquiring the data streams. SubVIs and drivers specific to the DAQ are used to manage the acquisition. LabVIEW first establishes communication between the computer and the DAQ. LabVIEW then specifies channels used and the scan rate for the analog inputs, as well as the analog outputs used for temperature and electric field measurements.

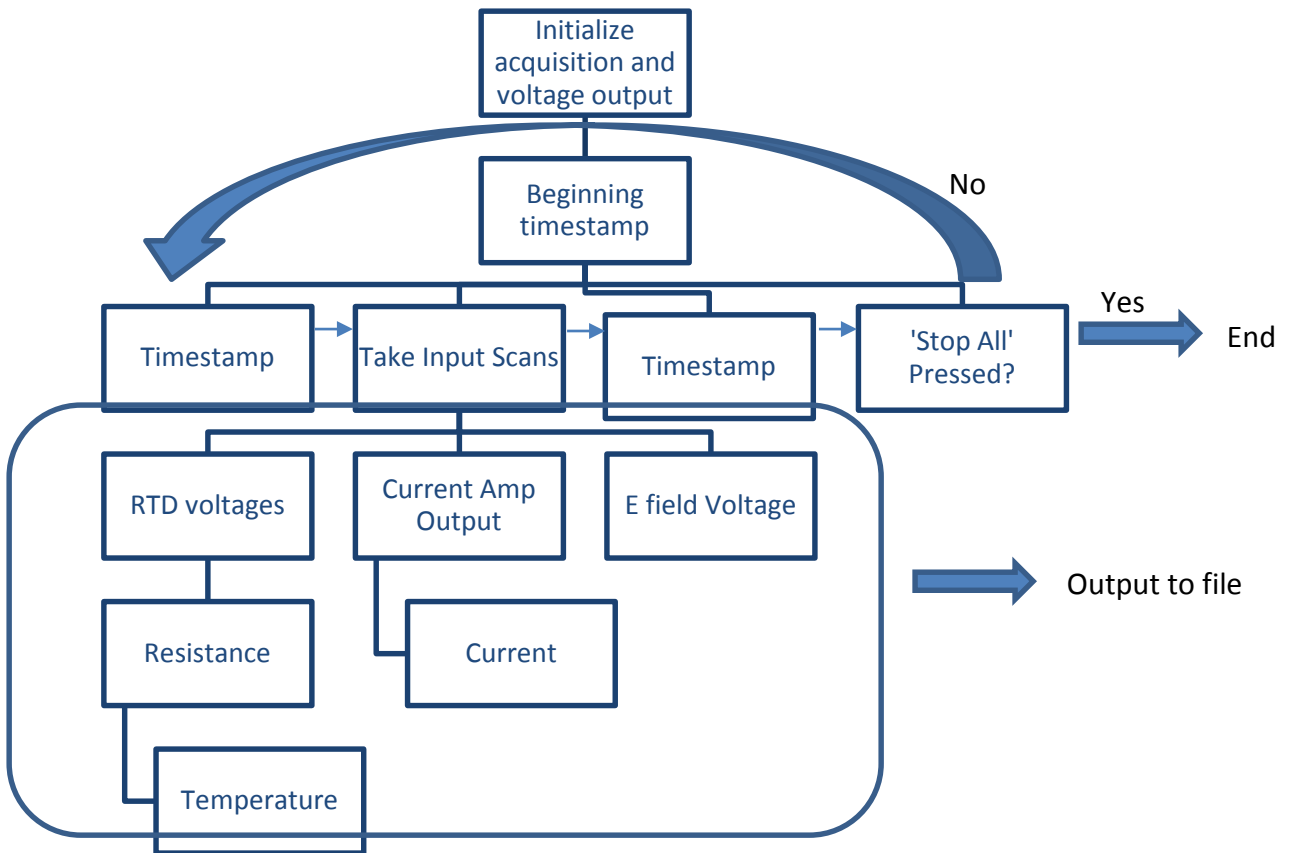


Fig. 12 The data acquisition subprocess. There is initialization in the beginning before the DAQ continuously takes readings that are then processed during the run and saved in the end.

Two analog output channels are used. One is for the application of electric field, which is controlled in the heater subprogram, and the other is for reading the temperature of the sample. The latter analog output acts as a voltage source for the voltage divider circuit used to read the resistance of the RTD chip.

Four analog input channels are used. Two are for the RTD voltage divider circuit; one reads the analog output voltage source, while the other reads the voltage over the constant resistor. From these measurements and the known constant resistance, the subprogram calculates the current resistance of the RTD chip and uses that to calculate the current temperature of the sample. Since the initial resistance of the RTD chip is not consistent, there is an offset input that can be used to calibrate the temperature calculation. The third analog input channel is used to read the voltage of the electric field on the sample straight from the analog output channel. The fourth channel is the voltage output of the current amplifier, which is then multiplied by the current amplifier gain to give the current from the sample

The analog input channels are read together at a user-specified scan rate. These scans are then used for the temperature and current calculations. A waveform chart is also used for real-time analysis, and consists of the resistance of the RTD chip, the calculated temperature, the current, and the applied voltage. The timing is determined by incrementing from the first time stamp by the timing of the scan.

The current amplifier subprocess is used for changing the gain, the filter, and the gain mode of the current amplifier, and recording the time the changes occur. It uses subVIs specific to the current amplifier. It first establishes communication to the current amplifier, and then sets the gain for pyroelectric current, the filters inside the amplifier, and the gain mode. It will then look for changes in the user inputs for the amplifier and implement the changes as needed, recording the times they occur. Since the gain change for the electric field is done in the heater subprocess, when the value of the electric field gain is changed, the current amplifier subprocess only records the time the value change occurred.

4.4 Synchronization

The efficiency of the pyroelectric energy conversion cycle is dependent on the precise timing of the temperature and electric field cycles. LabVIEW is used to manage the timing of the cycle. As each subprocess is in parallel, all the subprograms are asynchronous to each other. For example, the heater, DAQ, and current amplifier subprocesses initialize communication with the equipment and set up parameters in the beginning; the heater process, however, will pause and not continue until the ‘Start Heat’ button is pressed, while the DAQ and current amplifier subprocesses will continue immediately after initialization. This way, the operation of the DAQ and the current amplifier can be checked before the heating cycle is started. To end all subprocesses, the ‘Stop All’ button should be used.

Once the heater subprocess starts one of the heating modes, it will use that mode until the option input is changed. Toggling the electric field is also seen as changing the mode, which means that enabling or disabling the electric field in Timed mode will reset the cycle to the first step of letting the temperature reach a threshold before starting the periodic cycle. This will be altered in future iterations of the program. In Manual mode, the electric field will not be enabled or disabled until the next time the ‘Heat Off’ button is pressed, unless the electric field was enabled before the ‘Start Heat’ button was pressed. Temp mode is not affected by the mode being changed.

The electric field subVI has its own specific timing that can be modified by the user during runtime. The current timing scheme is described in Fig. 13.

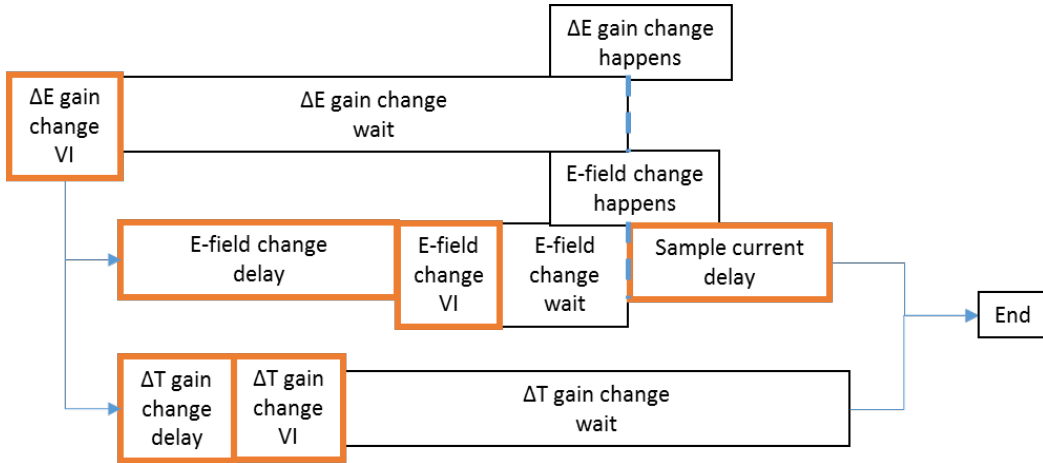


Fig. 13 Electric field subVI timing. The orange boxes are actual subVIs, while black boxes represent how long they take to occur.

There is a delay between sending the command to change the gain to the current amplifier, and the gain change actually occurring. When this change occurs, there are voltage spikes in the amplifier output. This calls for delays after calling the changes in gain in the subVI to keep the electric field change within the window of the electric field gain, which can be changed by the user during runtime to help with debugging. These delays also have to be overlapped to keep this window as small as possible, so as to not lose too much data on the pyroelectric current in the meanwhile.

Multiple parameters can be changed while the program is running. This includes the magnitude of the electric fields, the voltage to the heater, the period and duty of the timed heating cycle, the current amplifier parameters, the temperature thresholds for the Temp and Timed modes, the delays for gain switching, the offset for temperature calculation, and the file path for the output data file. However, none of the analog input parameters can be changed during the run, including the scan rate, nor the analog output channels.

4.5 Saving Data

After the ‘Stop All’ button is pressed, all subprocesses will end, and data will be saved in a .csv file, with its name and location specified by the user. The data contained include the parameters for the heater power supply; the offset for the temperature calculation; the initial gain settings; all the scans from the DAQ; the resistance, temperature, and current calculated from the scans; and timestamps for the scans. It also includes the timestamps for the heating cycle, times and values for whether or not the current amplifier settings or the heater voltage were changed during runtime, and timestamps from the electric field subVI.

5. Results

The goal of this work was to create a pyroelectric energy conversion testing setup to evaluate the performance of pyroelectric devices. Beginning with static ferroelectric materials characterization, the test setup was built up with components of increasing complexity toward realizing complete conversion cycles.

5.1 Static Testing

The pyroelectric sample was tested under static temperature conditions using the heater element and a Radian Precision Premier II Ferroelectric Tester to estimate the conversion cycle output. The hysteresis loops at 2 different temperatures are compared in Fig. 14. The isothermal polarization-electric field data can be used to represent 2 of the 4 conversion processes and, thus, estimate the energy conversion properties. At the baseline temperature, the dielectric displacement, leakage current, and capacitance are measured. The capacitance measurement is shown in Fig. 15, while the leakage current is shown in Fig. 16. The sample was then heated, the temperature was stabilized, and the hysteresis measurement was performed a second time.

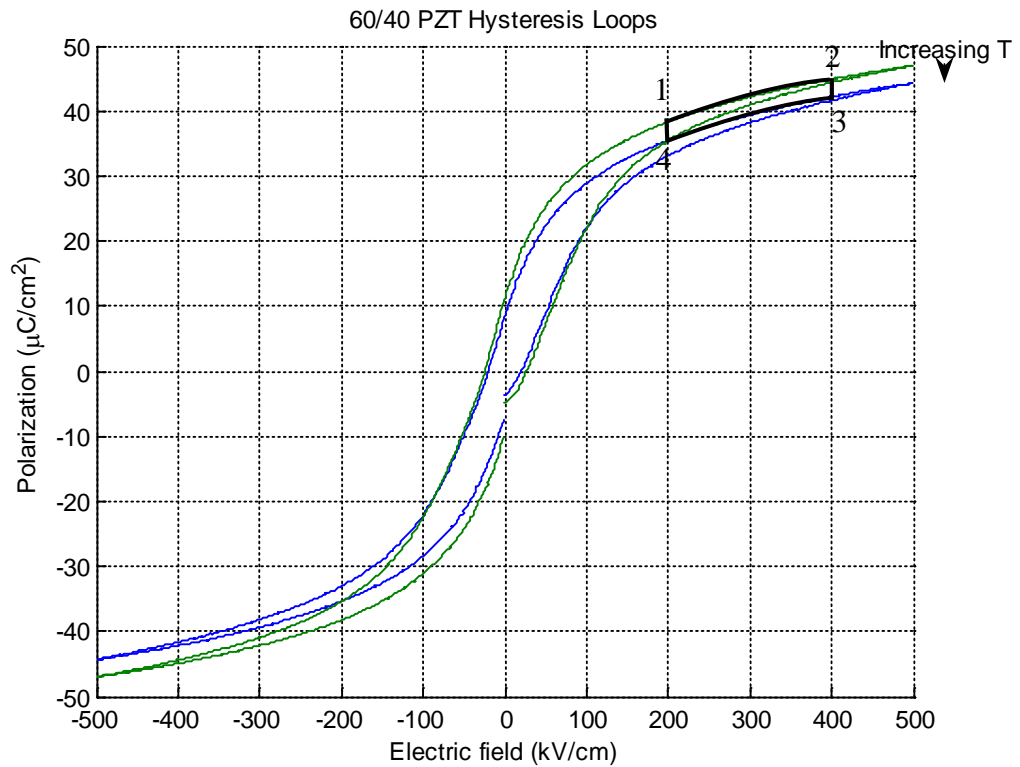


Fig. 14 Two hysteresis loops at a cold temperature and a hot temperature. The upper curves of the loops between points 1 and 2, and 3 and 4 represent the adiabatic charging and discharging of the Brayton cycle, while the differences in the loops at a constant voltage between points 2 and 3, and 4 and 1 represent the isoelectric heating and cooling.

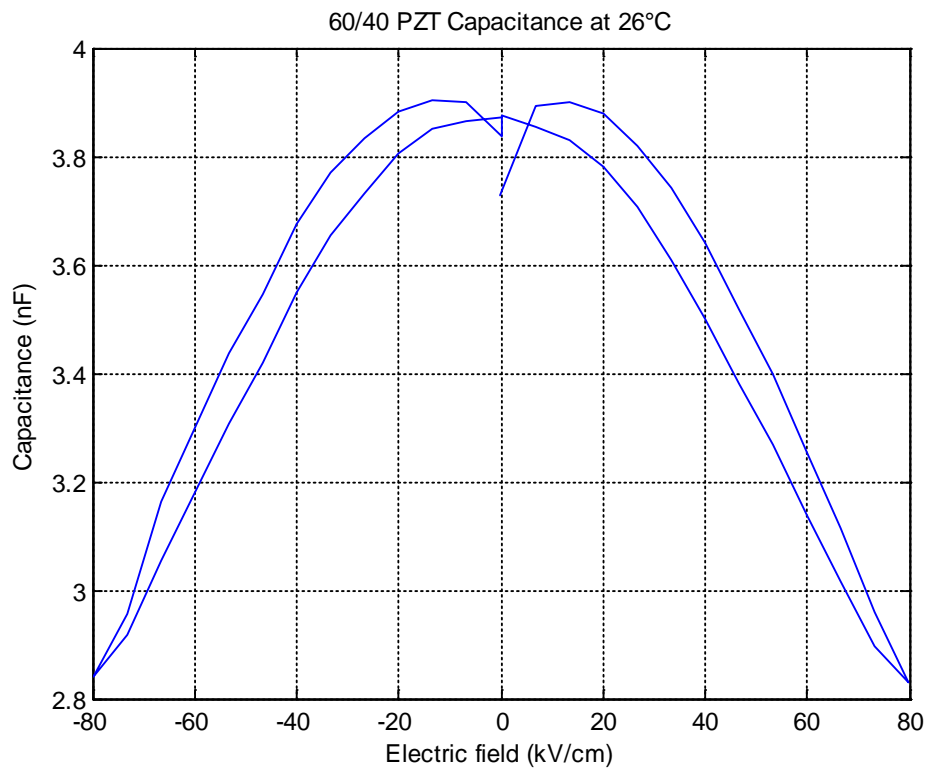


Fig. 15 Capacitance versus voltage for the pyroelectric sample at the cold temperature

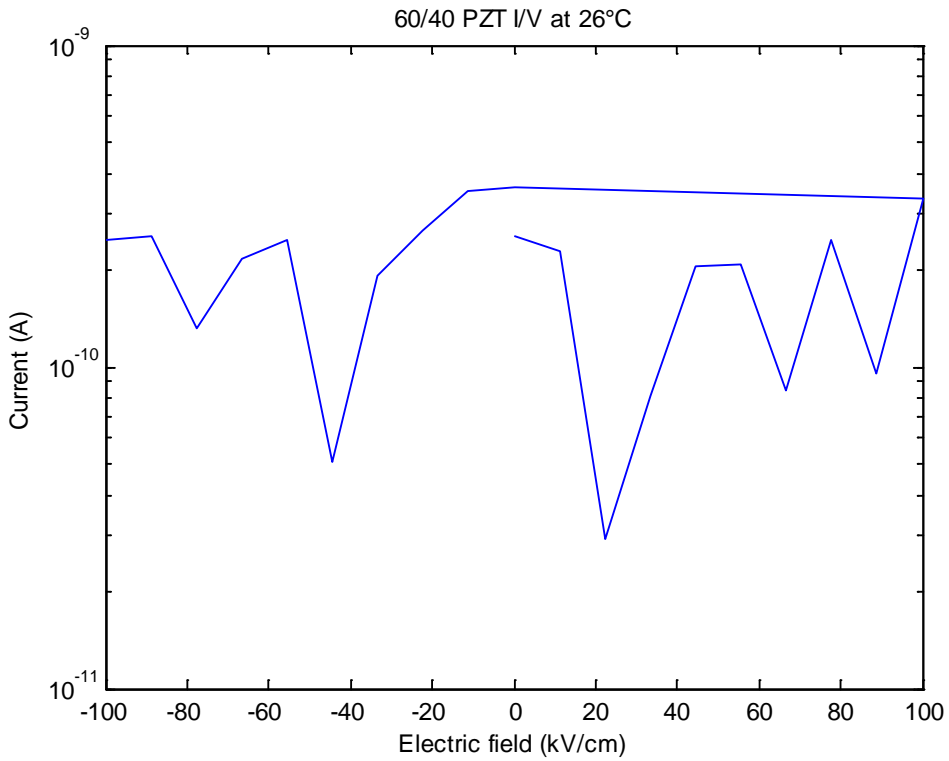


Fig. 16 The leakage current of the pyroelectric sample at the cold temperature. The heating rate has to be fast enough to have the pyroelectric current be visible past the leakage current.

5.2 Temperature Characterization

The RTD chip's resistance increases linearly with temperature, so it can be used as a temperature sensor. To determine the actual relationship, the chip was placed on the heater in the probe station, and the temperature controller ramped the temperature of the RTD chip up and down while the resistance was measured using the voltage divider circuit and the DAQ.

A frequent problem during testing was that the initial measured resistance changed with the landing of the probes on the chip. This is shown in Fig. 17. When the initial resistance was off from the typical value, the slope and offset of the temperature relationship would also be off. One solution was to ramp the heat before testing. As it cooled to its original temperature, the resistance often corrected itself and matched the correct slope and offset more closely. Ramping the temperature multiple times without lifting the probes led to more confident measurements.

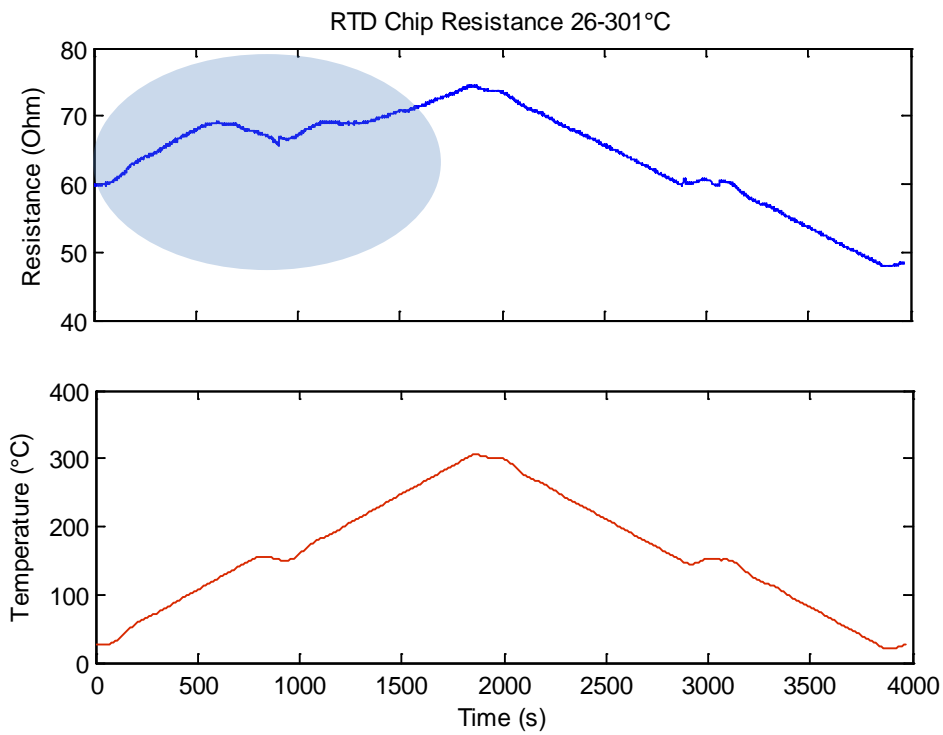


Fig. 17 Resistance and temperature over time. The humps highlighted in the beginning of the resistance plot is caused by poor contact between the probes and the RTD chip.

Thermal grease was added between the stage of the probe station and the ceramic heater, and between the heater and the RTD chip to improve thermal contact. This increased the slope of the relationship, meaning the contact resistance was reduced.

The ceramic resistive heater is controlled by enabling and disabling the voltage of a DC power supply, with the temperature controller setting the probe station at a baseline temperature. The performance of the heater showed a typical exponential heating curve. When the heater was on, the temperature would increase rapidly at first before plateauing at a high temperature determined by the balance of heating power in and cooling power out. When the heater turned off, the temperature would decrease quickly before slowing as it approached the cold plate temperature. The temperature controller would be trying to maintain the baseline cold plate temperature during this process. The cold plate heating power initially required to keep the baseline would decrease, and eventually dropped to zero if the heater element was cycled repeatedly at a frequency beyond the reaction time of the cold plate. When the heater element was turned off, the system temperature would drop significantly because of the flowing liquid nitrogen within the cold plate until the Lakeshore temperature controller brought it back to the baseline temperature.

Fast temperature cycles are required for efficient pyroelectric energy conversion. This makes only the initial increases and decreases of the exponential heating curve optimal, which forms a triangle-like temperature waveform. When the frequency of the waveform is held constant, the offset of the waveform will decrease as the temperature controller attempts to maintain the baseline temperature until it achieves maximum cooling. If the temperature offset and amplitude are held constant instead, the period of the waveform will increase, as it takes longer to reach those temperatures.

5.3 Pyroelectric Current

Accurate measurements of very low currents (<nA) are required to evaluate small pyroelectric devices undergoing relatively slow temperature variations (<1 Hz). Some issues appeared when first applying heat to the pyroelectric sample without any applied electric field. Crosstalk was visible both in the voltage divider measurements and in the current amplifier output, which was coming from the heater as the heater voltage was enabled and disabled. This was solved by covering the heater with indium foil that contacted with the sample stage, and putting the sample and RTD chip on top of that. This created a Faraday cage to shield the sample and RTD from the heater. Crosstalk was further reduced by moving the connections to the DAQ around so that the input channels in use were not so close together.

Pyroelectric current was visible with the current amplifier connected to the top of the pyroelectric capacitor and the ground of the capacitor connected to common ground (Fig. 18). As expected, it was about 90° out of phase with the temperature waveform. The current switched signs when the temperature switched from heating to cooling, and the current was maximum during the constant slope of the triangle temperature waveform. There is some minor deviation from the thermal and current waveforms being perfectly 90°, likely caused by the fact that the current and temperature measurements came from 2 different chips, which could have slightly different thermal contact properties.

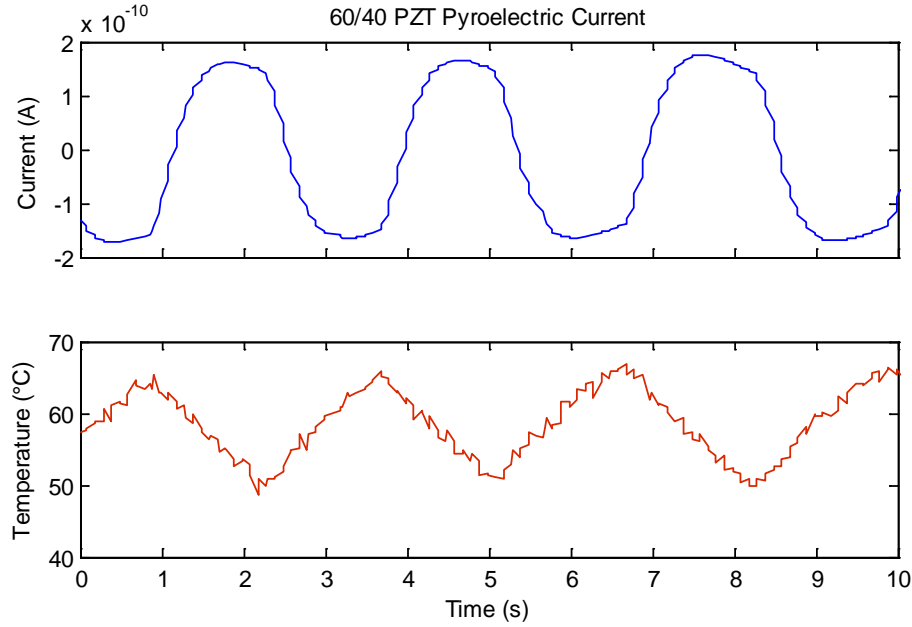


Fig. 18 Pyroelectric current with triangle temperature waveform. It is clear that it is pyroelectric because it is consistently the expected shape, it is about 90° out of phase with the temperature, and it is on the order of magnitude expected.

There are multiple inputs in the LabVIEW program that need to be determined before beginning the program. For communication purposes, the program needs the instrument addresses of the heater power supply and the current amplifier. The DAQ requires the scan rate and the total scans taken at a time for the analog input readings, and the channel numbers for the analog inputs and outputs. The heater power supply requires a voltage amount for the heater, as well as a current limit and a voltage protection limit. The current amplifier requires 2 gain values. One will be the gain set during pyroelectric current measurements, while the other will be the gain for measuring dielectric charging and discharging current.

The electric field is applied by connecting the ground of the pyroelectric capacitor to an analog output of the DAQ. The DAQ will output 0 V through that channel until other specified. When the electric field first turns on, the current amplifier will output a voltage spike as the capacitor first charges. The electric field will then cycle high and low, which causes the capacitor to charge and discharge, respectively. During this process, the gain of the current amplifier is switching repeatedly (as described in Section 4) to read the pyroelectric current and the charging/discharging current. The gain switching causes voltage spikes in the current amplifier output. The amplifier output may also drop to zero while changing gain. This behavior helps indicate when the gain is being changed, so that the data collected during these periods can be discarded.

The shape of the pyroelectric current changes with the addition of the electric field, as expected. This is because the electric field influences the polarization of the sample, meaning the amount of charge that will move due to the temperature change varies depending on the electric field.

5.4 Pyroelectric Energy Conversion Cycle Testing

At the maximum voltage of the heater power supply of 40 V, the fastest heating rate possible is about 10° per second. When the Brayton cycle is run with the testing setup, the results are as seen in Fig. 19.

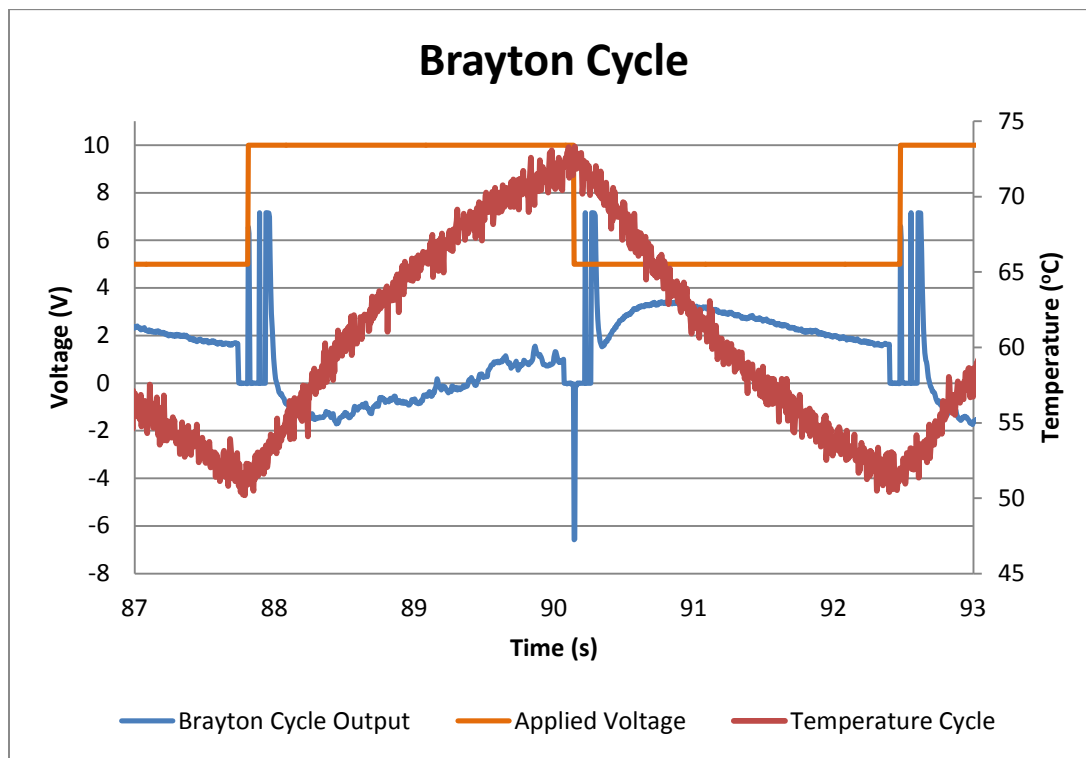


Fig. 19 A graph of the Brayton cycle. The Brayton cycle output is the voltage output of the current amplifier, so it shows the shape of the output current but not the exact value. The applied voltage is for the electric field.

Figure 19 shows a complete Brayton cycle. Adiabatic charging begins when the temperature is at its minimum. The charging causes a positive spike, which is followed by more spikes from the current amplifier as it changes to a more sensitive gain. There is then negative pyroelectric current as the sample goes through isoelectric heat addition. At the maximum temperature, the output zeroes out at the gain is changed before the adiabatic discharging, which causes a negative spike. The gain changes back to the sensitive gain, and there is a positive current as the sample goes through isoelectric heat loss.

The voltage spikes representing the adiabatic charge and discharge are clipped at the amplifier's max output, as they were measured at too sensitive a gain. They will then give an incorrect current when converted. To convert the current amplifier voltage output to current, it has to be multiplied by the gains the current amplifier was set at when the measurements were taken. The voltage spikes caused when the current amplifier changes the input gain also should be discarded from the data set. This is seen in Figs. 20 and 21.

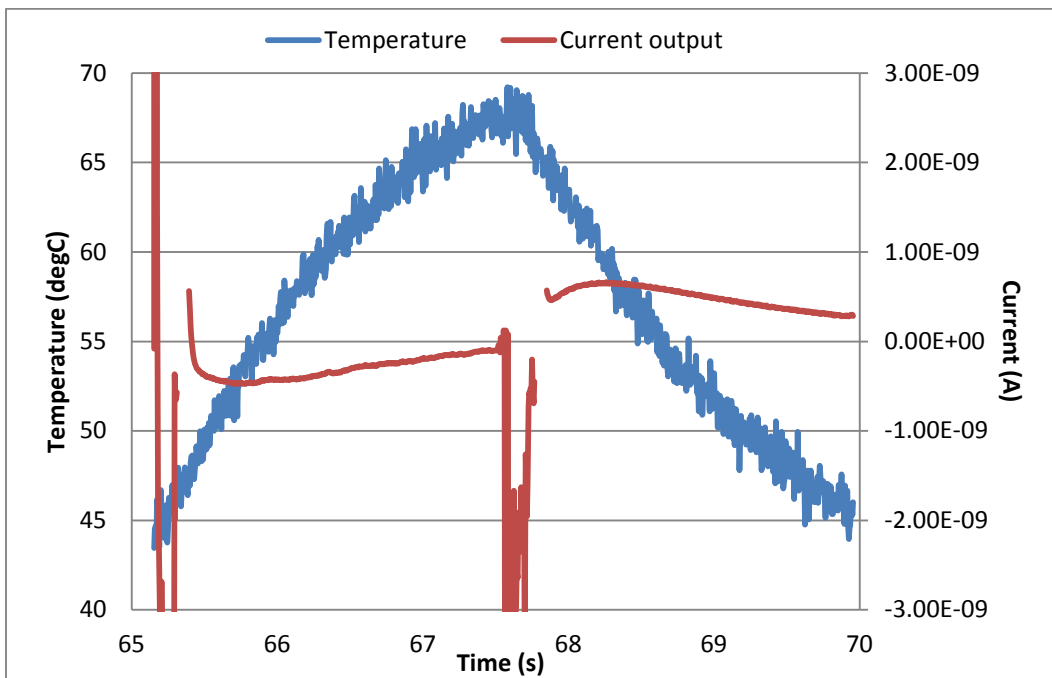


Fig. 20 Brayton cycle current, specifically the pyroelectric current. The spikes from the adiabatic charge and discharge are not shown in full. The temperature curve is shown as well. Some data were discarded due to voltage spikes occurring when the current amplifier changes gain.

One issue with discarding data is determining how much should be removed. For example, it is possible that some data left in are from the current amplifier output coming down from voltage spikes caused by the gain change instead of being pyroelectric current.

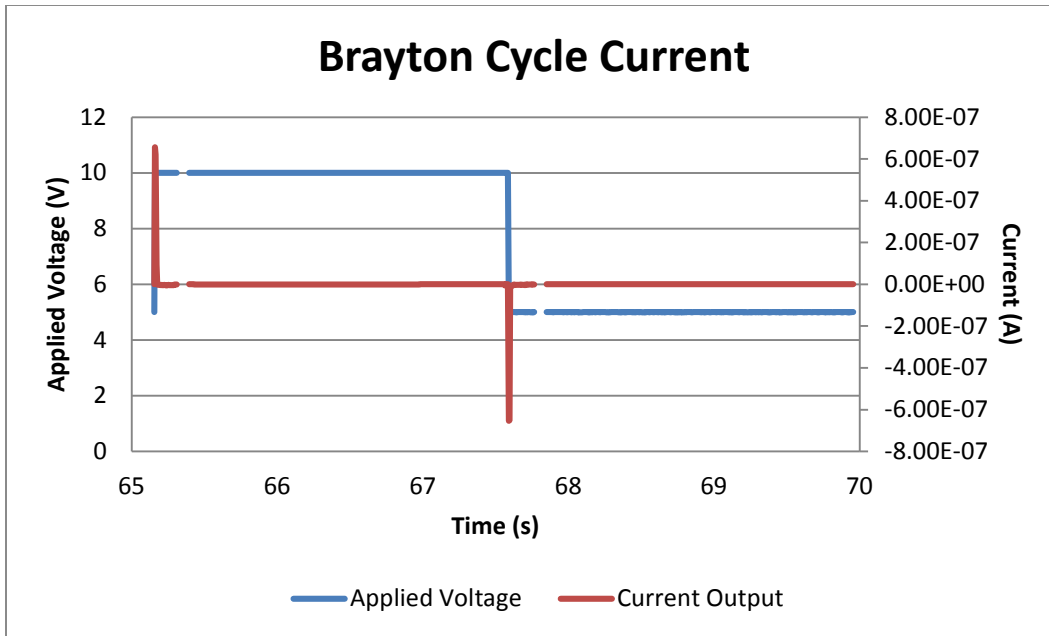


Fig. 21 Brayton cycle current, specifically the dielectric charge and discharge events. The currents at those points are incorrect, as the voltage output was clipped there. Some data were discarded due to voltage spikes occurring when the current amplifier changes gain.

As seen in Fig. 21, there is a positive spike in the current during the adiabatic charging. The current then becomes several orders of magnitude lower and negative during the isoelectric heating. A more negative current spike by orders of magnitude happens during the adiabatic discharging, and the current then becomes positive and orders of magnitude lower during the isoelectric cooling.

The static measurements of the Brayton cycle consist of the 2 hysteresis loops at 2 different temperatures, which are in displacement versus electric field. To convert the current measurements of the Brayton cycle to displacement, the current needs to be integrated to get charge, and divided by the area of the pyroelectric capacitor. The displacement can then be graphed against the applied electric field, which is the applied voltage divided by the thickness of the pyroelectric sample. The graph would then match the hysteresis loop graphs.

Figure 22 is an estimation of the Brayton cycle. It uses the pyroelectric current data seen in Fig. 20.

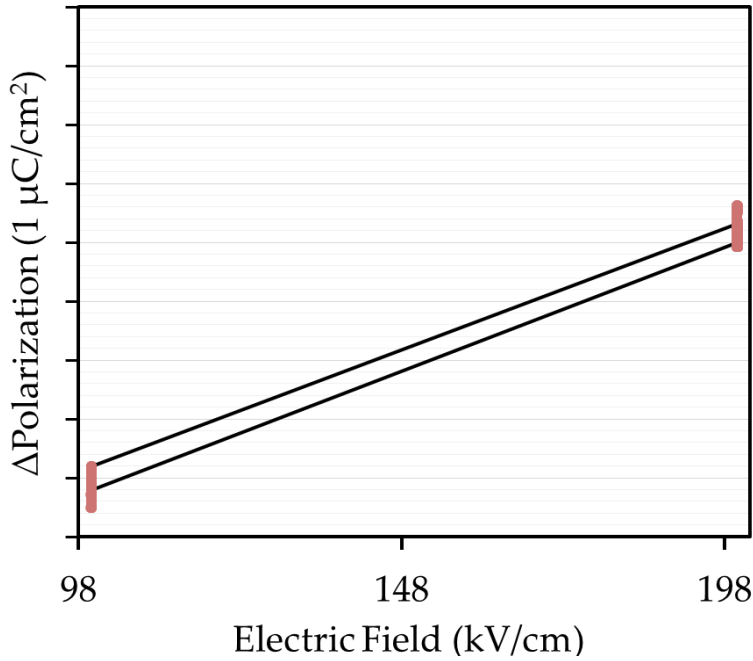


Fig. 22 Pyroelectric energy conversion loop calculated from current measurements

The area of the D-E graph of a Brayton cycle is the work done. That means the greater the temperature changes or the electric field differences, and the closer to the Curie temperature at which the cycle occurs, the more energy is converted. A faster cycle frequency would then increase the total power.

6. Conclusion and Future Outlook

The pyroelectric energy conversion cycle can be manipulated by a number of factors, including the electric field magnitudes and the temperatures the cycle uses. With a more complex test setup, these factors could be tested more thoroughly.

The pyroelectric testing setup should be able to handle any pyroelectric sample and heating method, and multiple improvements are necessary to make this happen. One current issue is the speed of the testing available. Faster temperature swings mean more pyroelectric current and energy output, making it necessary to be able to run faster Brayton cycles when quicker heating methods become available. This would include speeding up the program and the data reading itself, as needed.

Another possibility is including a high voltage amplifier in the setup so that the electric field can be increased past what the DAQ can output. A higher electric field means a greater change in electric field available, which would also increase the energy output of the cycle. The voltage amplifier would go between the DAQ analog output and the probe station where the sample is housed. A voltage divider

could possibly be used to connect the amplifier output to the DAQ, so the DAQ could read a scaled voltage within its ± 10 V input range and convert that to the actual greater applied voltage.

The noise level is something that also could be improved. Lower noise would increase the accuracy of the data, especially with the low voltage readings. Also, noise in the electric field could cause current from the slight resulting charge and discharge of the capacitor. Lower noise would reduce this.

In the future, the goal is to use a pulsed laser as a heating source and use the high voltage amplifier for an electric field. This will give greater energy and power outputs than what is currently possible. Another goal is to eventually test multiple samples and compare their Brayton cycle performances.

7. References

- Batra AK, Bandyopadhyay A, Chilvery AK, Thomas M. Modeling and simulation for PVDF-based pyroelectric energy harvester. *Energy Science and Technology*. 2013;5(2):1–7.
- Bhatia B, Damodaran AR., Cho H, Martin LW, King WP. High-frequency thermal-electrical cycles for pyroelectric energy conversion. *Journal of Applied Physics*. 2014;116(19):194509. doi:doi:<http://dx.doi.org/10.1063/1.4901993>
- Jankowski N, Smith A, Hanrahan B. (2016, July 10–14, 2016). Thermal model of a thin film pulsed pyroelectric generator. Paper presented at the ASME 2016 Summer Heat Transfer Conference, Washington, D.C.
- Lee FY, Jo HR, Lynch CS, Pilon L. Pyroelectric energy conversion using PLZT ceramics and the ferroelectric–ergodic relaxor phase transition. *Smart Materials and Structures*. 2013;22(2):025038. doi:10.1088/0964-1726/22/2/025038
- Navid A, Vanderpool D, Bah A, Pilon L. Towards optimization of a pyroelectric energy converter for harvesting waste heat. *International Journal of Heat and Mass Transfer*. 2010;53(19–20):4060–4070. doi:10.1016/j.ijheatmasstransfer.2010.05.025
- Olsen RB, Bruno DA, Briscoe JM. Pyroelectric conversion cycles. *Journal of Applied Physics*. 1985;58(12):4709. doi:10.1063/1.336244
- Sebald G, Guyomar D, Agbossou A. On thermoelectric and pyroelectric energy harvesting. *Smart Materials and Structures*. 2009;18(12):125006. doi:10.1088/0964-1726/18/12/125006
- Sebald G, Pruvost S, Guyomar, D. Energy harvesting based on Ericsson pyroelectric cycles in a relaxor ferroelectric ceramic. *Smart Materials and Structures*. 2008;17(1):015012. doi:10.1088/0964-1726/17/01/015012

1 DEFENSE TECH INFO CTR
(PDF) DTIC OCA

2 US ARMY RSRCH LAB
(PDF) IMAL HRA MAIL & RECORDS MGMT
RDRL CIO LL TECHL LIB

1 GOVT PRNTG OFC
(PDF) A MALHOTRA

2 US ARMY RSRCH LAB
(PDF) RDRL SED E
B HANRAHAN
F SZE

INTENTIONALLY LEFT BLANK.